

Calibration of selected bulk biomaterials parameters for DEM simulation of comminution process. Case study: corn and rice grains

Weronika Kruszelnicka^{1*}, Jan Diviš^{2,3}, Jakub Hlosta^{2,3}, Łukasz Gierz^{4*}, David Žurovec³

¹ Bydgoszcz University of Science and Technology, Faculty of Mechanical Engineering, Department of Machines and Technical systems, Al. Prof. S. Kaliskiego 7, 85-793 Bydgoszcz, Poland
werkru001@pbs.edu.pl (W.K.)

² VSB – Technical University of Ostrava, CEET, ENET Centre, Bulk Solids Centre, 17. listopadu 15/2172, 708 00 Ostrava-Poruba, Czech Republic
jakub.hlosta@vsb.cz (J.H.)

³ VSB – Technical University of Ostrava, Faculty of Mining and Geology, Department of Mining Engineering and Safety, 17. Listopadu 15/2172, 708 00 Ostrava-Poruba, Czech Republic
jan.divis@vsb.cz (J.D.); david.zurovec@vsb.cz (D.Ž.)

⁴ Poznan University of Technology, Institute of Machine Design, Faculty of Mechanical Engineering, ul. Piotrowo 3, 60-965 Poznan, Poland
lukasz.gierz@put.poznan.pl (Ł.G.)

*Corresponding author

Abstract

Computer simulation of bulk materials behavior, including comminution and fragmentation, using DEM has been growing fast, recently. One of the important tasks to get the reliable simulation results is to provide proper materials and contact parameters, which need to be determined in a series of laboratory experiments. For comminution simulation the additional parameters describing the breakage probability and breakage functions are necessary. While some simulation parameters are available in the literature for brittle materials, valid data are lacking for biomaterials such as cereal, rice or corn grains, especially for comminution parameters. The aim of this study was to present the calibration approach and determination of materials, contact, interaction and breakage parameters for grainy biomaterials. The calibration process was done for rice and corn grains. The calibration approach consists of grains size distribution and shape characterization, friction and restitution coefficient determination, and breakage probability description. Based on the results of the experiments, the models were created in the DEM software. The result was the set of calibrated parameters for rice and corn grains.

Keywords

DEM, comminution, angle of repose, restitution coefficient, breakage probability, biomaterials

1. Introduction

The computer simulation of the behavior of bulk materials, including comminution and fragmentation, using DEM has been growing rapidly recently. One of important tasks to obtain reliable simulation results is to provide proper materials and contact parameters, which needs to be determined in a series of laboratory experiments. For a comminution simulation, additional parameters are necessary to describe the probability of breakage and breakage functions are necessary. While for brittle materials some simulation parameters are available in the literature for the probability [1] and statistical crack characteristics [2], for biomaterials such as cereals, rice, or corn grains, there is a lack of valid data, especially for comminution parameters.

Biomaterials, also called biological resources, show considerable diversity [3], even within a species [4], which makes it difficult to model machines and devices for processing in terms of efficiency [5] and energy consumption [6]. Obtaining information about the properties of materials is a basic step in the analysis of their processability, in particular the probability of cracking and the cracking function. Many works are devoted to ecological aspects that define the relationship between the processed plant material, the machine's working units, and the processes involved. Understanding these relationships contributes to improved process efficiency [7], maintaining the good quality of the final product [8], reducing energy consumption [9], and the amount of waste generated [10] along with their neutralization according to the principles of sustainable development [11]. Furthermore, the assumptions of economy 4.0 [12] emphasize the importance of efficient and sustainable use of resources [13], including cereals considered the basis of food security [14].

Currently, among cereals, it is maize [15] and rice [16] that are the most important crops and raw materials in the world; they can also be classified as the most productive [17]. They are the main source of food, feed, and raw materials in many areas. Among cereal crops, maize is the largest cultivated area in the world and is the most processed material [18], while rice is the staple food of 1/3 of the world's population [19] and therefore plays an important role in the agri-food industry [20]. The correct selection of the operational parameters of the equipment to cut, harvest [21] and processing (e.g., shredding) these plants [22] guarantees the knowledge of the mechanical properties of the stalks [23], cobs, ears, and kernels [24] also fragmented [25] of both maize [26] and rice [27]. In previous studies, the selected mechanical properties of corn kernels and the fracture energy were determined [28]. It has also been empirically confirmed that the mechanical properties that cause the fracture, such as force, energy, and stress, depend on the grain size and, more precisely, on the thickness [28]. While analyzing the literature, one can find works devoted to the influence of the drying process of grains on their hardness and susceptibility to grinding [29], but also works that ambiguously describe the method of calculating and measuring the energy of the fracture. However, they do not indicate to what moment of fracture they refer to in accordance with the ASAE S368.4 DEC2000 (R2008) [30] standard.

For the improvement of DEM simulation models, it is necessary to obtain reliable data conditioning the accuracy of the simulation test results [31]. The interaction properties

important in DEM modeling are the restitution coefficients [32], static and rolling friction [33] and the angle of repose [34].

The scientific literature still lacks models describing the probability of breakage of various kernels, in particular maize and rice kernels, which are the most important food, feed, and energy in the world.

There are still few research centers involved in the study of the physical and mechanical properties of grains, and the available ones differ in the methods used and the test conditions. When grinding cereal grains, for example, in wheat, an increase in fracture energy was observed with increasing mass [3] (greater grain thickness, greater force and thus the energy necessary for grinding) [5]. The subsequent available work [35] ambiguously describes how the fracture energy was measured (or calculated). In the scientific literature, there have been attempts to describe the probability of fracture of materials using known distributions taking into account the influence of moisture [36] also comparatively for two types of maize [37]. However, these results take into account hard materials, especially minerals [38] and rocks [39], but also the cracking of droplets [40]. There are still no parameters for biological (cereal) materials such as rice or corn.

The purpose of this study was to present the calibration approach and determination of materials, contact, interaction, and breakage parameters for grainy biomaterials, in particular for corn grains and rice.

2. Materials and methods

In this study, the input parameters for DEM modeling of bulk materials (rice and corn) comminution were determined and the calibration procedure was shown as well. The research included both an experimental part and a simulation approach using RockyDEM software (see Figure 1). The calibration approach consists of characterization of grain size and shape, determination of the coefficient of friction and restitution, and description of the breakage probability (Figure 1). Based on the experimental results, the models were developed in the DEM software. The result was the set of calibrated parameters for rice and corn grains.

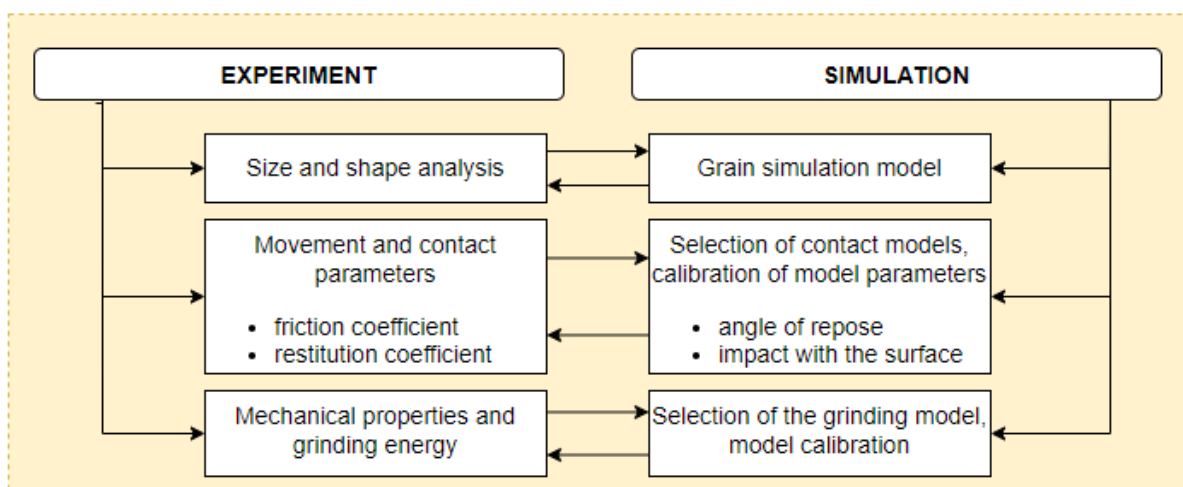


Fig. 1. Scope of the research

2.1. Particle size and shape characterization

The grains used in this study were rice and corn, which are commonly available for sale. The grains were pre-cleaned before the tests. The moisture content of the corn grains was 12.234% and of the rice grains 11.342%. For determination of size and shape, the particle size analysis was performed using the Camsizer device according to ISO standard 13322-2:2006 [41]. As a result, a cumulative distribution of particles size was obtained. Additionally, images of the grains were taken under stereoscopic microscope OptaTech with 15x zoom.

Then, 100 grains of rice and corn were selected and their dimensions (width (W), height (H) and length (L)) and mass were measured using an electronic caliper. The selected grains were further subjected to compression tests.

2.2. Static and rolling friction

The test apparatus shown in Figure 2 was used to measure the static friction between particulate materials and the wall material. This is a simple experiment, simulating the decomposition of forces on an inclined plane, where first a particle is placed on a fixed wall material and then the wall material sample is slowly tilted until the particle is set in motion. This moment is recorded and a digital protractor is used to read the angle of tilt at which the gravitational force component of the particle overcomes the frictional force that has held it stationary up to that point. The coefficient of static friction between the particle and the contact material μ_{s-pw} is determined from the measured angle α_{s-pw} using the equation [42]:

$$\mu_{s-pw} = \tan(\alpha_{s-pw}) \quad (1)$$

The problem arises with grains with a spherical or cylindrical shape. That is, grains that have a much lower coefficient of rolling friction than static friction. These will start to roll off the wall material much sooner than slide. This effect needs to be eliminated by gluing some particles together. With a particle surface formed in this way, the free rotation of the grains is prevented and only static friction is measured, not rolling. To determine the static friction between two particles μ_{s-pp} the same procedure was used, replacing the wall material sample with another particle surface.

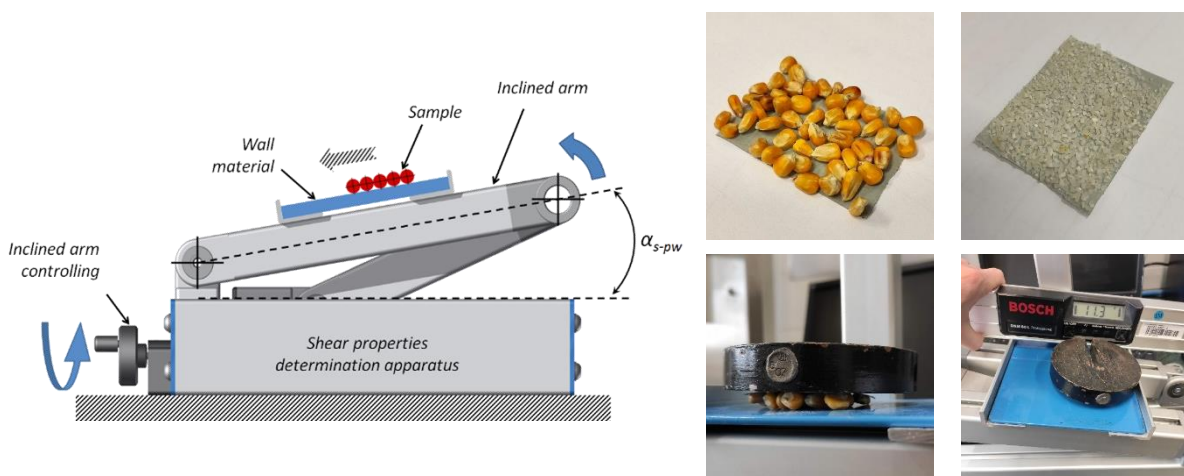


Fig. 2. Static friction coefficient experimental determination

The coefficient of rolling friction is a discussed topic among DEM modelers, as evidenced by the number of publications dealing with this issue [43, 44]. The same measurement methodology as for the static friction coefficient was also used for the rolling friction coefficient μ_r . Due to the variety of particle shapes, it was not possible to determine the coefficient of rolling friction completely and accurately for all corn and rice particles. The coefficient of rolling friction was therefore used as a variable calibration parameter in the repose angle tests. For contact models in DEM, the coefficient of rolling friction is a function of particle shape, not a material property. This issue is discussed in publications such as Wensrich and Katterfeld (2012) [43]. They argue that shape plays an important role in the behavior of particulate materials, but unfortunately it is one of the properties that is very difficult to model accurately [43]. Rolling friction provides a simple way to introduce particle shape-based behavior into a model, but there are many open questions associated with this technique for now.

2.3. Restitution coefficient

The coefficient of restitution is the ratio of the final to the initial relative velocity between two objects after they collide. It usually vary from 0 to 1, where 1 would be a perfectly elastic collision. The coefficient of restitution can be thought of as the degree to which the mechanical (kinetic or potential) energy of bodies is conserved when they bounce off a surface or another body [45]. Thus, in general:

$$e_{pw} = \sqrt{\frac{E_{\text{Kinetic (after collision)}}}{E_{\text{Kinetic (before collision)}}}} = \sqrt{\frac{\frac{1}{2}mv_2^2}{\frac{1}{2}mv_1^2}} = \sqrt{\frac{v_2^2}{v_1^2}} = \frac{v_2}{v_1} \quad (2)$$

The particle collision experiment on a double pendulum described by Hlosta et al (2018)[45] was used to determine the coefficient of restitution of two particles. Particle A placed on the pendulum suspension is released from the height h_1 . At the lower position, particle A collides with particle B. It thus transfers its kinetic energy to particle B, which bounces on the pendulum to height h_2 . The coefficient of restitution of the two particles can then be determined from the heights or velocities of the particles on the pendulum before and after the impact. Experiments were recorded with the Olympus i-Speed 2 high-speed camera at 500 fps and a resolution of 800x600 px with i-Speed tracking software. The positions of the tracked particles over time were exported using the tracking software and processed by a spreadsheet. At a frame rate of 500 fps, 150-200 data points were acquired for each measurement. This means that the length of the evaluated process was 0.3-0.4 s. The recordings were evaluated and the heights and velocities were determined. The calculation uses the particle velocities immediately before and after the impact, i.e., essentially the maximum particle velocities. Three experiments were performed for each pair of particles.

The same method was used to measure the particle-boundary restitution coefficient. One particle pendulum was replaced with a static sample of wall material. The bounce height and velocity of one particle were measured. A schematic of the measurement of the restitution coefficient is shown in Figure 3.

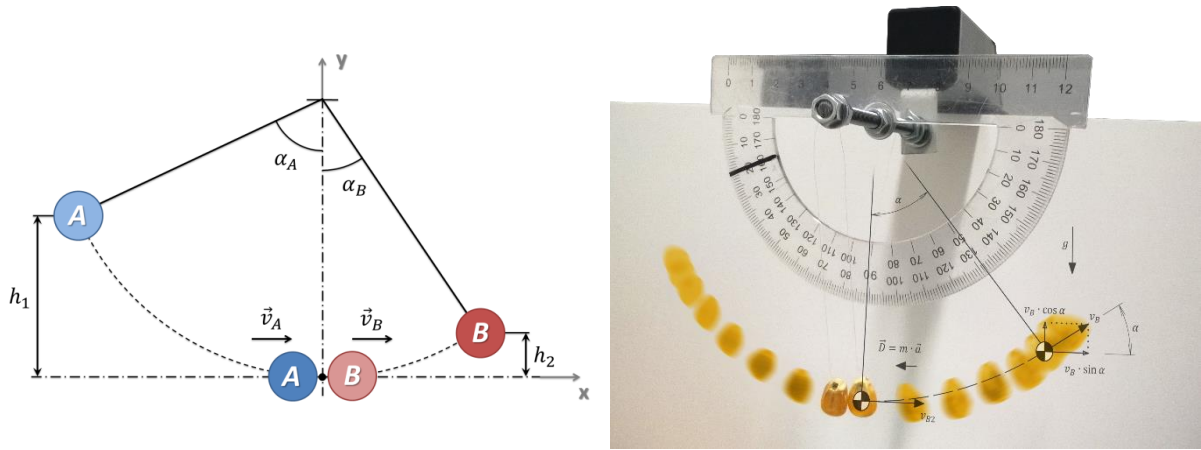


Fig. 3. Restitution coefficient experimental determination

2.4. Angle of repose

In this work, calibration using static and dynamic repose angle was chosen as the calibration DEM method. Calibration using the static angle of repose is primarily used to optimize interparticle interaction parameters. For the calibration via the dynamic angle of repose, a rotating drum was used with the static friction between particles and a steel cylinder.

The drum diameter of 140 mm corresponds to approx. 20 corn particles across the flow surface profile. An adequate number of particles is important for determining the angle of repose. A low number of particles may lead to distorted results. Similarly, if there are too many particles in the drum, the DEM calculation times increase significantly. As some materials travel in different ways in the drum, their trajectories were in all cases compared with the recordings of the experiment. This comparison allowed for the evaluation of whether a material could be retained with existing properties or if any of the parameters needed to be adjusted [42].

2.5. Breakage probability

Computer modeling of comminution can be realized if the proper input parameters about breakage of grains are known. In the commercial software (ex. RockyDEM) there are some built in breakage models, such as Ab-T10 - model which calculates the breakage probability distribution based on the value of cumulated contact energy [46] and Tavares breakage model which is based on the upper-truncated log-normal probability distribution of specific fracture energy [47–49]. The breakage probability model is described by the equation [47–49]:

$$P_0(e) = \frac{1}{2} \left[1 + \operatorname{erf} \left(\frac{\ln e^* - \ln e_{50}}{\sqrt{2\sigma^2}} \right) \right] \quad (3)$$

where: P_0 – breakage probability, e^* – relative particle specific fracture energy, e_{50} – median particle specific fracture energy, σ^2 – variance of the log-normal distribution of fracture energy.

In the above equation, the e_{50} shows the dependance between the medians of the lognormal distribution of breakage probability for particle in different sizes and is described by the equation [47–49]:

$$e_{50} = \frac{e_{\infty}}{1 + \frac{k_p}{k_{st}}} \left[1 + \left(\frac{d_0}{d_p} \right)^{\varphi} \right] \quad (4)$$

where: e_{∞} , d_0 and φ are the model parameters that should be adjusted to the experimental data, and d_p is a representative particle size for a given size class, k_{st} is the steel stiffness (230GPa) and k_p is particle stiffness.

The empirical data to describe breakage probability was obtained based from the compression test results. The 100 grains of known size (as described in the section 2.1) were compressed on an Instron 5966 and MTS criterion model 43 universal testing machine (according to ASAE S368.4 standard [30]) and the force and displacement were measured. As well, the influence of moisture content (MC) of breakage probability was assed. In this case the 100 grains from grains with different MC levels, it is 10,14, 18, 22 and 26% were compressed. To obtain the comparable samples the grains were firstly rewetted to 28% MC and then dried in the room temperature to the desired level of MC. The energy values during compression of one grain is the area under graph $F=f(D)$. The energy required to destroy the grain was determined based on Eq. (5) [1, 50-51]:

$$E_{(RP)} = \int_{D_1}^{D(RP)} F dD \quad (5)$$

where: $E_{(RP)}$ – energy input until occurrence of rupture point (RP), J, F – force, N, dD – deformation corresponding to RP, mm.

According to Tavares et al. [1], mass specific energy corresponding to the points $E_{m(RP)}$ was determined based on equation:

$$E_{m(RP)} = \frac{1}{m} \int_{D_1}^{D(RP)} F dD = \frac{E_{(RP)}}{m} \quad (6)$$

where: m – mass of a single grain expressed in kilograms.

In order to determine cumulated probability distributions of specific energy, their values were structured in an ascending order ranking $i = 1, 2 \dots N$, for particular observations. Cumulated empirical probability distribution of the analyzed property can then be determined from a dependence resulting from the Hanzen score method [2, 51]:

$$P(X_i) = \frac{i - 0.5}{N} \quad (7)$$

where: $P(X_i)$ – value of cumulated distribution of probability of a given property occurrence, X_i defines the analyzed property (specific energy), and N is the number of observations.

The empirical distributions were determined for grains divided into 4 size classes according to the height of the single particles, so it was possible to get the values of medians of the lognormal distributions for different size class. The Levenberg-Marquardt nonlinear optimization

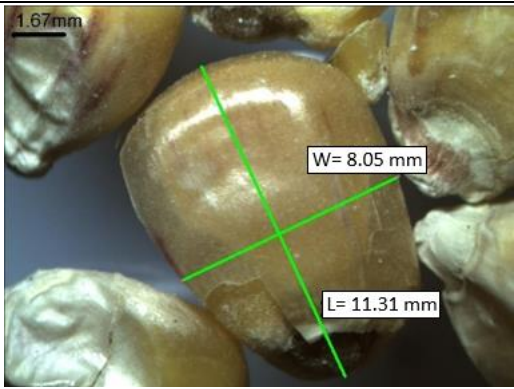
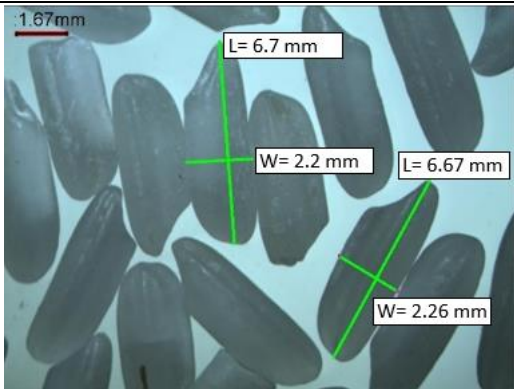
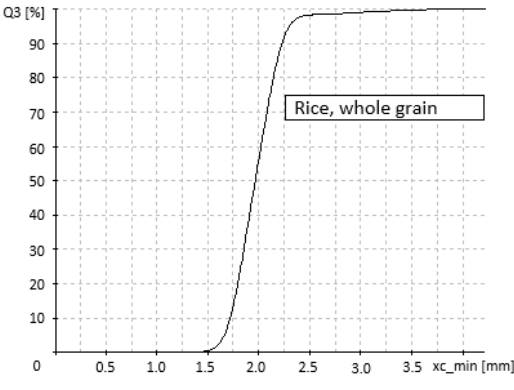
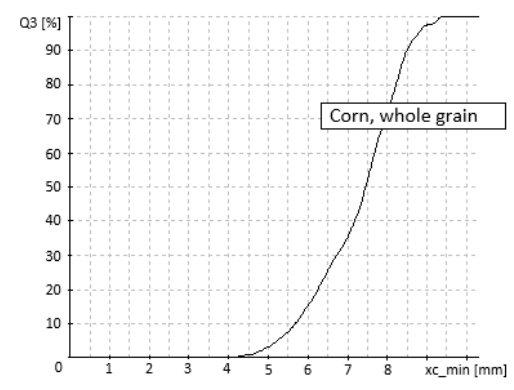
algorithm was used to fit the probability distributions and describe the relationship between e_{50} and particle size.

3. Results and discussion

3.1. Particle size and shape characterization

Table 1 shows the results of particle size and shape characterization. The corn grains were characterized by higher sphericity than rice grains, which have more prolonged shape. The average width of corn grains was equal to 7.85 mm, the average length was 10.65 mm and the average height was 4.88 mm. For rice it was 1.91 mm, 6.38 mm, 1.51 mm for the width, length and height, respectively. The median size of the cumulative distribution for corn was 7.48 mm and for rice 1.67 mm.

Table 1. Results of particle size and shape characterization

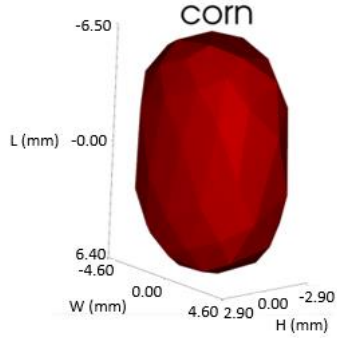
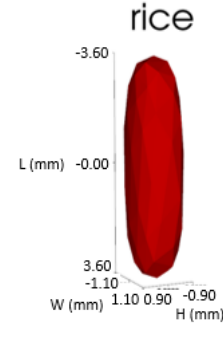
	Corn			Rice		
Image	 <p>Medium sphericity, rounded edges, shiny hull surface;</p>			 <p>Low sphericity, prolonged shape, rounded edges, smooth surface</p>		
Particle size distribution						
Single particle dimension	L [mm]	W [mm]	H [mm]	L [mm]	W [mm]	H [mm]
Average	10.65	7.85	4.88	6.38	1.91	1.51
Median	10.72	7.90	4.78	6.40	1.94	1.50
St. dev.	0.91	0.82	0.52	0.55	0.18	0.11

L – length, W – width, H – height, Q3 – cumulated distribution based on volume, xc_min – diameter of particle which is the shortest chord of the set of measured maximum chords

The above data was used to create the virtual model of the particles. The particle shape was created based on the polyhedral shape available in the RockyDEM software. The specific shape parameters such as vertical aspect ratio, horizontal aspect ratio, number of corners and superquadratic degree were determined based on the data from Table 1 and bulk density

calibration in the cylindrical container. Table 2 present the calibrated size and shape parameters for corn and rice grains.

Table 2. Calibrated particle size and shape for DEM simulation

Corn				Rice			
							
Material shape		Material size		Material shape		Material size	
		Sieve size, mm	Cumulative, %			Sieve size, mm	Cumulative, %
Vertical Aspect Ratio	0.62	9.76	100	Vertical Aspect Ratio	0.80	2.27	100
Horizontal Aspect Ratio	1.36	8.45	79	Horizontal Aspect Ratio	3.30	2.10	93
Number of Corners	60	7.85	47	Number of Corners	60	1.93	48
Superquadric Degree	3.00	7.22	21	Superquadric Degree	3.00	1.70	15
		6.58	3				

3.2. Static friction

In the DEM simulation of bulk materials such as cereals grains the important parameters are those characterizing their behavior in contact with surface or other particles. One of the most common is the static friction coefficient μ_{s-pw} . In table 3 the results of static friction coefficient determination for corn and rice grains against paint coated steel plate and plate without paint. Additionally, the μ_{s-pw} was determined for comminuted grains. It can be seen that for the paint coated steel plate the static friction coefficient was lower than for steel plate in all cases. It should be noted that the comminution of materials changes the values of μ_{s-pw} . In the tests with the paint coated plate, the μ_{s-pw} was lower for the crushed rice and corn grains than for these grains no subjected to comminution. For the steel plate without paint the adverse effect was observed – the μ_{s-pw} was higher for the crushed rice and corn grains.

Table 3. The results of static friction coefficient tests

Particles	Wall Material	Angle α_{s-pw}				Coefficient of Static friction (-)
		Test No.1 (°)	Test No.2 (°)	Test No.3 (°)	Avg. Angle (°)	
Corn	paint coated steel	11.2	9.8	13.1	11.4	0.20
Corn	steel	10.7	13.0	14.2	12.6	0.22

Corn - crushed	paint coated steel	11.1	10.6	9.0	10.2	0.18
Corn - crushed	steel	14.7	15.8	13.5	14.7	0.25
Rice	paint coated steel	10.2	9.9	12.6	10.9	0.19
Rice	steel	14.7	14.6	13.6	14.3	0.24
Rice - crushed	paint coated steel	11.4	8.5	10.4	10.1	0.17
Rice - crushed	steel	15.8	18.9	16.0	16.9	0.29

3.3. Restitution coefficient

The second important parameter determining the bulk materials behavior is coefficient of restitution e_{pw} . Table 4 shows the values of obtained e_{pw} in the tests including contact between two particles and contact between particle and steel plate. The e_{pw} for impact of two corn particles was equal to 0.81 and for rice particles it was 0.42. The coefficient of restitution e_{pw} for impact between grains and steel plate was 0.48 and 0.68 for corn and rice, respectively.

Table 4. The results of coefficient of restitution for rice and corn grains

Particle	Particle/ Wall Material	Coefficient of restitution e_{pw}			
		Test No.1 (-)	Test No.2 (-)	Test No.3 (-)	Avg. (-)
Corn	Corn	0.85	0.79	0.79	0.81
Corn	Steel	0.47	0.51	0.46	0.48
Rice	Rice	0.44	0.40	0.42	0.42
Rice	Steel	0.69	0.74	0.62	0.68

3.4. Angle of repose

After the measurement of size and shape and physical properties measurement the virtual model of the grain was built and the simulation of the angle of repose test was done to verify the reliability and prediction power of bulk materials behavior in motion. In DEM software the test for static and dynamic angle of repose tests were simulated. As initial parameters the restitution coefficients and friction coefficients presented in Tables 3 and 4 were used. However to get the final agreement between physical experiment and simulation results the values of static and dynamic coefficient of friction needed to be changed. In the Figure 4 the pile formation of rice and corn grains during physical tests and simulation was presented and in the Figure 5 the results of dynamic test.

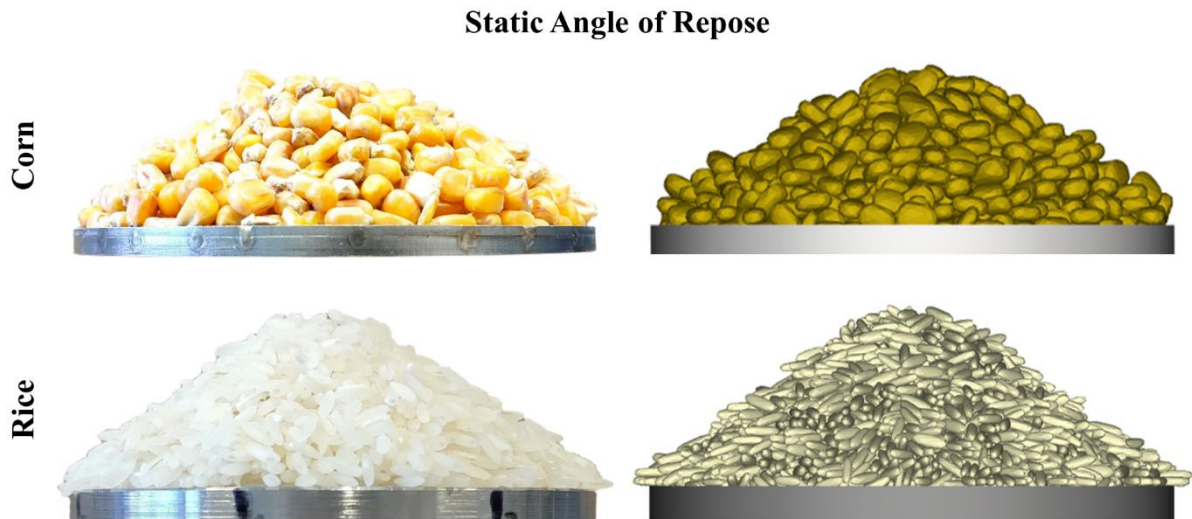


Fig. 4. The pile formation in the calibration of simulation parameters by static angle of repose (left – physical experiment, right – DEM simulation)

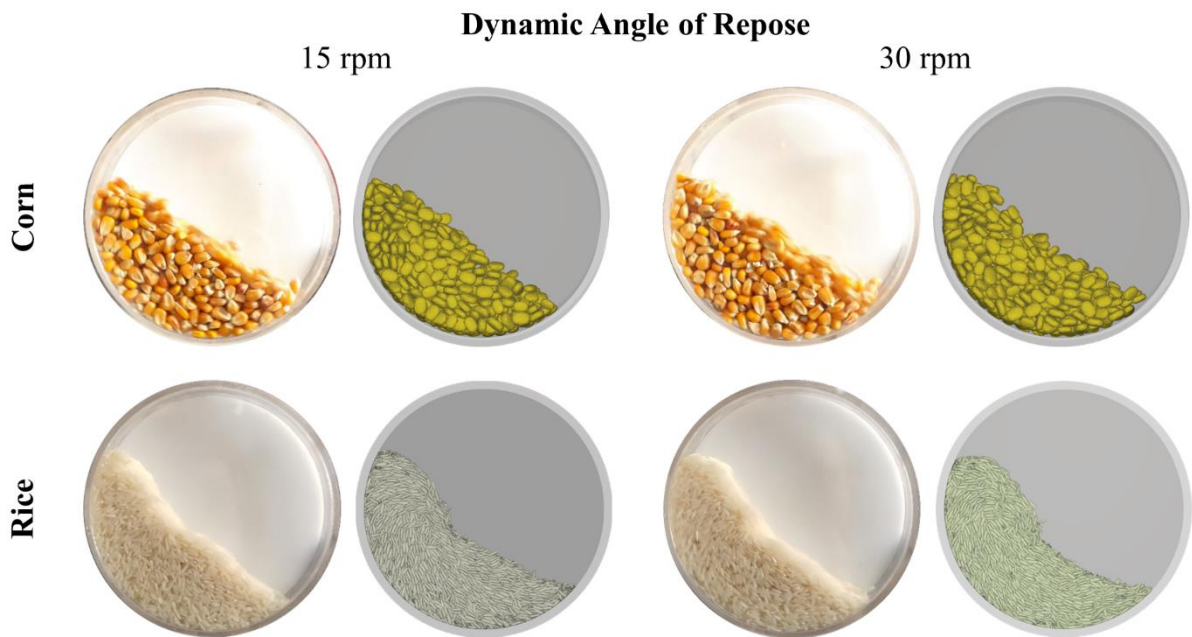


Fig. 5. The calibration of input parameters by dynamic angle of repose rotary drum test (left – physical experiment, right – DEM simulation)

As can be seen from the figures the built DEM simulation model is in agreement with physical experiment. While the shape of grains was not strictly mapped the friction coefficients used in the simulation are slightly different than presented in the previous sections. In the simulation the values of SFC for rice was 0.45 for interactions between particles and 0.42 for interactions between particle and surface. For corn the SFC which gives good agreement with physical experiment in the angle of repose test was 0.35 for particle-particle and particle-surface interactions. The dynamic friction coefficient for rice in particle-particle contact was set as 0.28 and in particle-surface interaction it was 0.35, for corn dynamic coefficient of friction was set on 0.22. The coefficient of rolling friction in the simulation was 0.01 and 0.05 for corn and rice grains, respectively. The values of static friction coefficient in the simulation, which provides

good agreement with physical experiment were higher for both, corn and rice grains, than values of static friction coefficient obtained on the experimental determination on shear properties apparatus. This confirms, similarly as in other previous research [52–54], that the simulation of bulk materials should be validated in specific bulk tests such as angle of repose, hopper discharge test and others, to adjust the physical properties determined based on the experiment.

3.5. Breakage probability

Figure 6 shows the breakage probability of corn and rice grains divided into four different size classes. The probability of grain damage under specific level of energy is higher for bigger particles for both corn and rice grains. It can be concluded that the statistical model of log-normal distribution could be used for breakage description of biomaterials grains, because of high values of R^2 coefficient (Table 5).

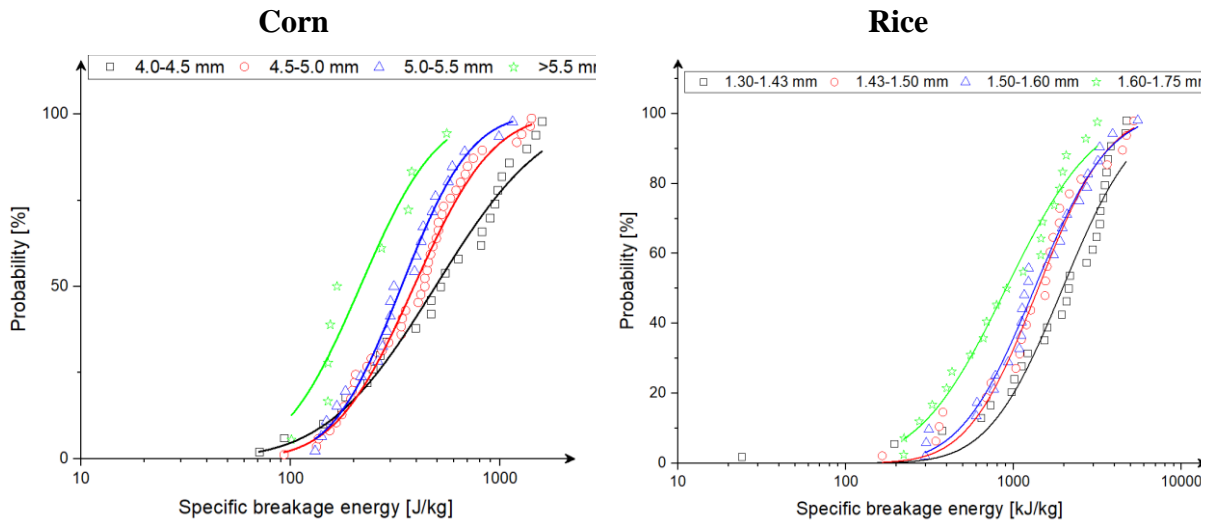


Fig. 6. Breakage probability and fitted curves of log-normal distribution

Table 5. The values of fitted log-normal distribution parameters

Corn			Rice		
Size range	Parameter	Value	Size range	Parameter	Value
4.0-4.5 mm	e_{50} [J/kg]	527.93	1.30-1.43 mm	e_{50} [J/kg]	1959.39742
	σ	0.94494		σ	0.79843
	R^2	0.9791		R^2	0.9557
4.5-5.0 mm	e_{50} [J/kg]	396.41	1.43-1.50 mm	e_{50} [J/kg]	1403.8459
	σ	0.685		σ	0.7538
	R^2	0.98473		R^2	0.9746
5.0-5.5 mm	e_{50} [J/kg]	341.21	1.50-1.60 m	e_{50} [J/kg]	1334.2235

	σ	0.60124		σ	0.7982
	R^2	0.9892		R^2	0.9826
>5.5 mm	e_{50} [J/kg]	220.79	1.60-1.75 mm	e_{50} [J/kg]	903.2919
	σ	0.65947		σ	0.9467
	R^2	0.9118		R^2	0.9797

The higher energy values were needed to initiate the breakage of smaller particles (see median values in Table 6 and Figure 7). This observation is similar as for brittle materials, such as rocks and minerals [1, 2, 51]. However, there is a risk that despite the promising statistical distributions of the fracture probability for single grains, such a good fit will not be achieved in the case of the particle set during grinding in the mill, which may cause discrepancies between the simulation and the experimental model.

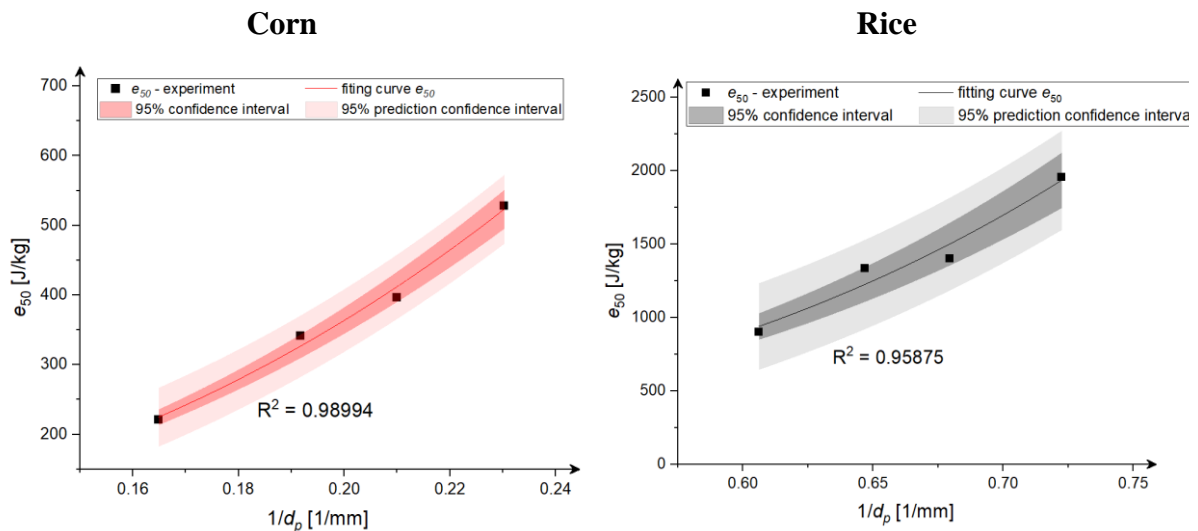


Fig. 7. The dependence between median energy e_{50} and particle size

Based on the medians obtained for the different size ranges of rice and corn grains it was possible to determine the values of coefficients used in equation (3) (Table 6). The analysis shows that the particle size and specific breakage energy are connected by a power function of particle size according to equation (4), as was presented in Figure 7. The high values of R^2 coefficient confirms the good agreement between the e_{50} model and experimental values, so it could be concluded that the method proposed by Tavares [47–49] to describe the breakage can be used also for biomaterials grains, however other factors such as moisture content should be also taken into account.

Table 6. Experimentally determined values of the parameters of the e_{50} model for corn and rice grains

Parameter	Corn	Rice
e_{∞} [J/kg]	26.87	31.81

k_p [MPa]	53.43	110.48
k_{st} [GPa]	230.00	230.00
d_0 [mm]	12.56	3.65
φ [-]	2.75	4.22

Figure 8 presents the breakage probability of grains for different moisture content. It can be seen that the probability of grain breakage varies for different moisture content, which confirms the necessity to include a moisture content as a parameter for breakage probability distribution function. In case of corn grains with 10% MC will break the most likely, while the grains with 26% MC will break the least likely subjected to the same energy level. For rice, the most likely to break was the grains with the 10% MC, but least likely will break the grains with 22% MC. It was observed that it is more likely that the grains with lower moisture content will brake subjected to the specific energy level than for grains with the highest moisture contents. So it can be said that the probability of breakage for these grain decrease with the increase in moisture content.

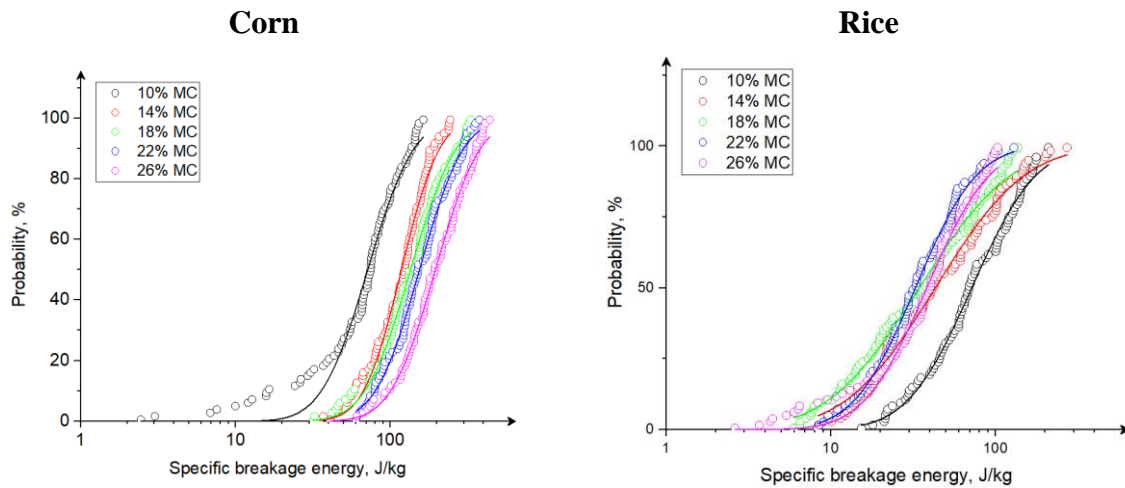


Fig. 8. Breakage probability distribution for different moisture content levels for rice and corn grains

Presented results are only partial description of the breakage parameters for DEM application, because it presents only the first approach presenting the breakage probabilities for different particle sizes, while the full procedure proposed by Tavares include the weakening process of grains subjected to repeated impacts and the particles size after breakage with the modification of Ab-t10 model. The approach including weakening is very time consuming and needs a high number of experiments and will be the subject of further research for development of DEM models of biomaterials grains.

4. Conclusions

In this study the set of parameters for DEM simulation for rice and corn grains was presented. The restitution coefficient for rice was 0.42 and 0.68 in particle-particle and particle-steel surface contact. For corn the restitution coefficient was equal to 0.81 and 0.48 in particle-particle and particle-steel surface contact, respectively. The static friction for particle and steel surface was 0.24 and 0.22 for rice and corn, respectively. It was found that for the paint coated steel plate the static friction coefficient was lower than for steel plate and that the comminution of materials changes the values of static friction coefficient. In the tests with the paint coated plate, the SFC was lower for the crushed rice and corn grains than for these grains no subjected to comminution. For the steel plate without paint the adverse effect was observed – the static friction coefficient was higher for the crushed rice and corn grains.

The values of static friction coefficient in the angle of repose test in DEM simulation, which provides good agreement with physical experiment were higher for both, corn and rice grains, than values of static friction coefficient obtained on the experimental determination on shear properties apparatus, which confirms that the parameters should be validated and verified individually, especially when the modelled shape of the particle is slightly different than real one.

It was found that the probability of grain damage could be described with the good agreement by the log-normal distribution. The study shows that under specific level of energy is higher for bigger particles for both corn and rice grains. It was found that higher energy values were needed to initiate the breakage of smaller particles and the particle size and specific breakage energy are connected by a power function of particle size. In the case of statistical models of breakage the further research should be conducted to determine the breakage probability in repeated impacts. The research shows that the breakage probability is dependent on the grain moisture content. In case of rice and corn it was found that the probability of breakage decrease with increase in MC. In the future studies the detailed research on the influence of MC on the breakage probability should be done, as well the universal model with moisture content as a parameter should be developed.

The determined parameters are of an application nature and can be used when designing processing machines dedicated to rice and corn. The knowledge of these values will allow, inter alia, to estimate the power of devices, e.g. crushers, roller and disc mills, and consequently to minimize energy losses and energy demand of dedicated machines.

Funding

This research was funded in whole or in part by National Science Center, Poland, grant number 2021/05/X/ST8/00114 under Miniatura V program and the National Center for Research and Development project number LIDER / 24/0137 / L-8/16 / NCBR / 2017.

Acknowledgments

We would like to thank the VSB – Technical University of Ostrava, CEET, ENET Centre, Bulk Solids Centre and Purdue University (USA) for research organization and provision of apparatus.

Weronika Kruszelnicka holds a scholarship (START 2022) and benefits from the financial aid of the Foundation for Polish Science (FNP) and here we would like to thank the Foundation for its support and patronage.

5. References

1. Tavares L.M., Cavalcanti P.P., de Carvalho R.M., da Silveira M.W., Bianchi M., Otaviano M. Fracture Probability and Fragment Size Distribution of Fired Iron Ore Pellets by Impact. *Powder Technol.* 2018, 336: 546–554.
2. Cavalcanti P.P., Tavares L.M. Statistical Analysis of Fracture Characteristics of Industrial Iron Ore Pellets. *Powder Technol.* 2018, 325: 659–668.
3. Wiercioch M., Niemiec A., Roma L. The impact of wheat seeds size on energy consumption of their grinding process. *Inżynieria Rol.* 2008, 103: 367–372.
4. Dziki D., Laskowski J. Influence of Wheat Kernel Geometrical Properties on the Mechanical Properties and Grinding Ability. *Acta Agrophys.* 2003, 2: 735–742
5. Kruszelnicka W., Bałdowska-Witos P., Kasner R., Flizikowski J., Tomporowski A., Rudnicki J. Evaluation of Emissivity and Environmental Safety of Biomass Grinders Drive. *Przem. Chem.* 2019, 98: 1494–1498.
6. Werechowska M. Some Physical Properties of Cereal Grain and Energy Consumption of Grinding. *Agric. Eng.* 2014, 1(149): 239–249
7. Atashbar N.Z., Labadie N., Prins C. Modelling and Optimisation of Biomass Supply Chains: A Review. *Int. J. Prod. Res.* 2018, 56: 3482–3506.
8. Jewiarz M., Wróbel M., Mudryk K., Szufa S. Impact of the Drying Temperature and Grinding Technique on Biomass Grindability. *Energies* 2020, 13: 3392.
9. Bembenek M. Exploring Efficiencies: Examining the Possibility of Decreasing the Size of the Briquettes Used as the Batch in the Electric Arc Furnace Dust Processing Line. *Sustainability* 2020, 12: 6393.
10. Hryniewicz M., Bembenek M., Janewicz A., Kosturkiewicz B. Brykietowanie materiałów drobnoziarnistych w prasach walcowych z niesymetrycznym układem zagęszczania. *Przem. Chem.* 2015, 94: 2223–2226.
11. Kovács Á., Kerényi G. Physical Characteristics and Mechanical Behaviour of Maize Stalks for Machine Development. *Int. Agrophysics* 2019, 33: 427–436
12. Winkler R. MeteoMex: open infrastructure for networked environmental monitoring and agriculture 4.0. *PeerJ Computer Science* 2021, 7: e343.
13. Aghi D., Mazzia V., Chiaberge M. Local motion planner for autonomous navigation in vineyards with a rgb-d camera-based algorithm and deep learning synergy. *Machines* 2020, 8: 27
14. Kumar R., Karmakar S., Minz A., Singh J., Kumar A., Kumar, A. Assessment of Greenhouse Gases Emission in Maize-Wheat Cropping System Under Varied N Fertilizer Application Using Cool Farm Tool. *Frontiers in Environmental Science* 2021, 9:710108.
15. Landoni M., Cassani E., Ghidoli M., Colombo F., Sangiorgio S., Papa G., Adani F., Pilu R. Brachytic mutation is able to counteract the main pleiotropic effects of brown midrib mutant in maize. *Scientific Reports* 2022, 12(1): 2446
16. Rodrigo D., Rosell C.M., Martinez A. Risk of *Bacillus cereus* in Relation to Rice and Derivatives. *Foods* 2021, 10: 302.
17. Soto-Gómez D., Pérez-Rodríguez P. Sustainable agriculture through perennial grains: Wheat, rice, maize, and other species. A review. *Agriculture, Ecosystems and Environment* 2022, 325: 107747
18. Chhabra, N. Kaur, A. Studies on Physical and Engineering Characteristics of Maize, Pearl Millet and Soybean. *J. Pharmacogn. Phytochem.* 2017, 6: 1–5.
19. Chandravarman P., Agyei D., Ali A. Green and sustainable technologies for the decontamination of fungi and mycotoxins in rice: A review. *Trends in Food Science and Technology* 2022, 124: 278-295

20. Kruszelnicka W. Study of Physical Properties of Rice and Corn Used for Energy Purposes. In Proceedings of the Renewable Energy Sources: Engineering, Technology, Innovation, Krynica, Poland, 20–22 June 2020, Wróbel, M., Jewiarz, M., Szlęk, A., Eds., Springer International Publishing: Berlin/Heidelberg, Germany 2020, 149–162.
21. Flizikowski J.B., Kruszelnicka W., Tomporowski A., Mrozinski A. A Study of Operating Parameters of a Roller Mill with a New Design. AIP Conf. Proc. 2019, 2077: 020018.
22. Kowalczyk-Juško A., Kowalczyk J., Szmigielski M., Marczuk A., Jozwiakowski K., Zarajczyk K., Maslowski A., Slaska-Grzywna B., Sagan A., Zarajczyk J. Quality of biomass pellets used as fuel or raw material for syngas production. Przem. Chem. 2015, 94: 1835–1837
23. Li Y., Qin T., Chen J., Zhao Z. Experiments and Analysis on Mechanical Property of Corn Stalk Reciprocating Cutting. Trans. Chin. Soc. Agric. Eng. 2011, 27: 160–164
24. Moya M., Aguado P.J., Ayuga F. Mechanical Properties of Some Granular Agricultural Materials Used in Silo Design. Int. Agrophysics 2013, 27: 181–193.
25. Chel-Guerrero L., Parra-Pérez J., Betancur-Ancona D., Castellanos-Ruelas A., Solorza-Feria J. Chemical, Rheological and Mechanical Evaluation of Maize Dough and Tortillas in Blends with Cassava and Malanga Flour. J. Food Sci. Technol. 2015, 52: 4387–4395.
26. Li W., Du Y., Liu L., Mao E., Yang F., Wu J., Wang L. Research on the constitutive model of low-damage corn threshing based on DEM, Comput. Electron. Agric. 2022, 194: 106722.
27. Tang Z., Li Y., Zhang B., Wang M., Li Y. Controlling Rice Leaf Breaking Force by Temperature and Moisture Content to Reduce Breakage. Agronomy 2020, 10: 628.
28. Kruszelnicka W. Study of Selected Physical-Mechanical Properties of Corn Grains Important from the Point of View of Mechanical Processing Systems Designing. Materials 2021, 14: 1467
29. Kim T.H. Physical Changes in Maize (*Zea mays* L.) Grains during Postharvest Drying, Massey University: Palmerston North, New Zeland, 2000, 239
30. American Society of Agricultural and Biological Engineers ASAE S368.4 DEC2000 (R2008): Compression Test of Food Materials of Convex Shape 2008
31. Gierz Ł., Kruszelnicka W., Robakowska M., Przybył K., Koszela K., Marciniak A., Zwiachel T. Optimization of the Sowing Unit of a Piezoelectrical Sensor Chamber with the Use of Grain Motion Modeling by Means of the Discrete Element Method. Case Study: Rape Seed. Appl. Sci. 2022, 12: 1594
32. LoCurto G. J., Zhang X., Zarikov V., Bucklin R. A., Vu-Quoc L., Hanes D. M., Walton O. R. Soybean impacts: Experiments and dynamic simulations. Trans. ASAE 1997, 40(3): 789-794
33. Chung Y. C., Ooi J. Y., Favier J. F. Measurement of mechanical properties of agricultural grains for DEM models. InProc. 17th ASCE Engineering Mechanics Conf. American Society of Civil Engineers, Newark, Del. 2004
34. Wang S., Yu Z., Aorigele, Zhang W. Study on the modeling method of sunflower seed particles based on the discrete element method. Computers and Electronics in Agriculture 2022, 198: 107012.
35. Lupu M.I., Pădureanu V., Canja C.M., Măzărel A. The Effect of Moisture Content on Grinding Process of Wheat and Maize Single Kernel. IOP Conf. Ser. Mater. Sci. Eng. 2016, 145: 022024.
36. Seifi M.R., Alimardani R. The Moisture Content Effect on Some Physical and Mechanical Properties of Corn (Sc 704). J. Agric. Sci. 2010, 2: 125.
37. Seifi M.R., Alimardani R. Comparison of Moisture-Dependent Physical and Mechanical Properties of Two Varieties of Corn (Sc 704 and Dc 370). Aust. J. Agric. Eng. 2010, 1: 170–178

38. Sun H., Zeng Y., Ye Y., Chen X., Zeng T. Abnormal Size Effect of Particle Breakage Probability under Repeated Impacts. *Powder Technol.* 2020, 363: 629–641.
39. Bwalya M.M., Chimwani N. Development of a More Descriptive Particle Breakage Probability Model, *Minerals* 2020, 10(8): 710
40. Maaß S., Kraume M. Determination of Breakage Rates Using Single Drop Experiments. *Chem. Eng. Sci.* 2012, 70: 146–164.
41. ISO ISO 13322-2:2006 Particle Size Analysis — Image Analysis Methods — Part 2: Dynamic Image Analysis Methods 2006
42. Hlosta J., Jezerská L., Rozbroj J., Žurovec D., Nečas J., Zegzulka J. DEM Investigation of the Influence of Particulate Properties and Operating Conditions on the Mixing Process in Rotary Drums: Part 1—Determination of the DEM Parameters and Calibration Process. *Processes* 2020, 8: 222.
43. Wensrich C.M., Katterfeld A. Rolling Friction as a Technique for Modelling Particle Shape in DEM. *Powder Technol.* 2012, 217: 409–417
44. Nečas J., Rozbroj J., Hlosta J., Diviš J., Kaprálek J., Žurovec D., Zegzulka J. Shear Lid Motion in DEM Shear Calibration and the Effect of Particle Rearrangement on the Internal Friction Angle. *Powder Technol.* 2022, 403: 117417.
45. Hlosta J., Žurovec D., Rozbroj J., Ramírez-Gómez Á., Nečas J., Zegzulka J. Experimental Determination of Particle–Particle Restitution Coefficient via Double Pendulum Method. *Chem. Eng. Res. Des.* 2018, 135: 222–233
46. Fengnian S., Kojovic T. Validation of a Model for Impact Breakage Incorporating Particle Size Effect. *Int. J. Miner. Process.* 2007, 82, 156–163.
47. Tavares L.M. Optimum Routes for Particle Breakage by Impact. *Powder Technol.* 2004, 142: 81–91.
48. Tavares L.M. Analysis of Particle Fracture by Repeated Stressing as Damage Accumulation. *Powder Technol.* 2009, 190: 327–339.
49. Tavares L.M., André F.P., Potapov A., Maliska C. Adapting a Breakage Model to Discrete Elements Using Polyhedral Particles. *Powder Technol.* 2020, 362: 208–220.
50. Sarker M.S.H., Hasan S.M.K., Ibrahim M.N., Aziz N.A., Punan Mohd. S. Mechanical Property and Quality Aspects of Rice Dried in Industrial Dryers. *J. Food Sci. Technol.* 2017, 54: 4129–4134.
51. Tavares L.M., de Almeida R.F. Breakage of Green Iron Ore Pellets. *Powder Technol.* 2020, 366: 497–507
52. Beakawi Al-Hashemi H.M., Baghabra Al-Amoudi O.S. A Review on the Angle of Repose of Granular Materials. *Powder Technol.* 2018, 330: 397–417.
53. Chen H., Zhao S., Zhou X. DEM Investigation of Angle of Repose for Super-Ellipsoidal Particles. *Particuology* 2020, 50: 53–66.
54. Wei H., Li M., Li Y., Ge Y., Saxén H., Yu Y. Discrete Element Method (DEM) and Experimental Studies of the Angle of Repose and Porosity Distribution of Pellet Pile. *Processes* 2019, 7: 561.